analytical chemistry

Article

pubs.acs.org/ac

Droplet-Based Microfluidic Flow Injection System with Large-Scale Concentration Gradient by a Single Nanoliter-Scale Injection for Enzyme Inhibition Assay

Long-Fei Cai,[†,‡] Ying Zhu,[†] Guan-Sheng Du,[†] and Qun Fang*[,†]

[†]Institute of Microanalytical Systems, Department of Chemistry, Zhejiang University, Hangzhou, 310058, China

[‡]Department of Chemistry, Hanshan Normal University, Chaozhou, 521041, China

Supporting Information

ABSTRACT: We described a microfluidic chip-based system capable of generating droplet array with a large scale concentration gradient by coupling flow injection gradient technique with droplet-based microfluidics. Multiple modules including sample injection, sample dispersion, gradient generation, droplet formation, mixing of sample and reagents, and online reaction within the droplets were integrated into the microchip. In the system, nanoliter-scale sample solution was automatically injected into the chip under valveless flow injection analysis mode. The sample zone was first dispersed in the microchannel to form a concentration gradient along the axial direction of the microchannel and then segmented into a linear array of droplets by immiscible oil phase. With the segmentation and protection of the oil phase, the concentration gradient profile of the sample was preserved in the droplet array with high fidelity. With a single injection of 16 nL of sample solution, an array of droplets with concentration gradient spanning 3−4 orders of magnitude could be generated. The present system was applied in the enzyme inhibition assay of β-galactosidase to preliminarily demonstrate its potential in high throughput drug screening. With a single injection of 16 nL of inhibitor solution, more than 240 in-droplet enzyme inhibition reactions with different inhibitor concentrations could be performed with an analysis time of 2.5 min. Compared with multiwell plate-based screening systems, the inhibitor consumption was reduced 1000-fold.

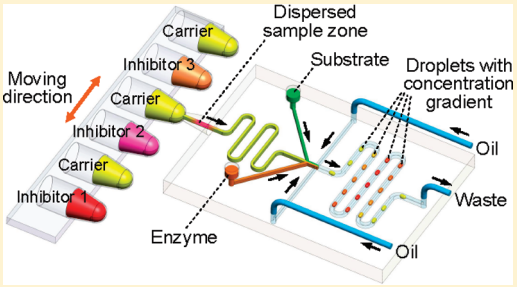

Recently, droplet-based microfluidics has emerged as a powerful platform for performing chemical and biological experiments in the picoliter to nanoliter range,[1−4] with the advantages of high-throughput, low sample and reagent consumptions, rapid mixing, and minimal cross-contamination. Benefiting from these features, droplet-based systems have been successfully applied in various fields such as cell-based assays,[5−7] enzyme kinetics,[8−10] protein expression,[11−14] and high throughput screening.[15−18]

Enzyme inhibition assays are frequently used in drug screening,[19,20] in which usually over thousands of compounds with different concentrations spanning 3−6 orders of magnitude are needed to be screened to find active inhibitors by measuring their inhibition efficiencies to a definite enzyme target. In conventional procedures, the test compound solutions with large concentration scale are prepared by sequentially diluting the stock solutions of the test compounds in manual mode or using robotics. Such operations are often time-consuming and labor intensive and have large sample and reagent consumptions in the microliter to milliliter range. Microfluidic systems hold great potential for enzyme inhibition assays in reducing the sample and reagent consumptions to the nanoliter range and generating a broad range of compound concentrations in microchannels. Currently, most of the microfluidic systems for generating concentration gradient were built on the basis of molecular diffusion across the multiphase laminar flows formed in microchannels.[21−23] In these systems, continuous flows of sample and reagents are required to be maintained to ensure a stable radial concentration gradient across the microchannel, which will lead to relatively large sample and reagent consumptions. Therefore, these systems may not be suitable for applications where only a small amount of compounds are available.

Droplet-based microfluidic systems provide an efficient way to generate concentration gradient since the concentration gradients can be maintained and confined in discrete picoliter to nanoliter droplets without dispersion. So far, there are four concentration-gradient generation modes in previously reported droplet-based microfluidic systems, including the continuous flow, multiphase laminar flow, batch dilution, and zone dispersion methods (Figure 1). Ismagilov's group[24,25] generated droplets with concentration gradient by continuously merging aqueous sample, reagent, and diluent streams at different flow rate ratios before droplet formation (Figure 1A). Several groups combined the laminar flow-molecular diffusion method with droplet formation to generate droplets with concentration gradient (Figure 1B).[26−28] In 2010, the authors'

Received: November 3, 2011
Accepted: November 30, 2011
Published: November 30, 2011

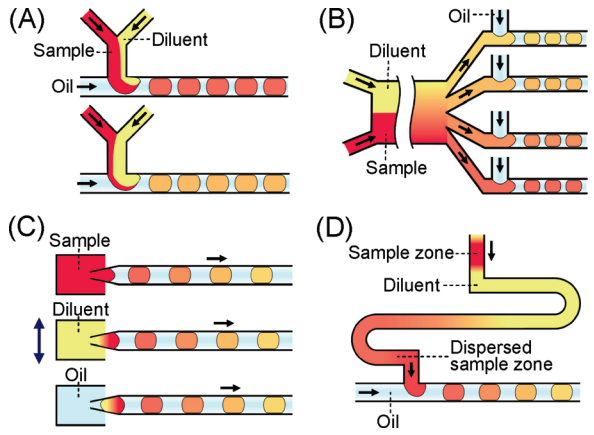

Figure 1. Various concentration-gradient generation modes in droplet-based microfluidic systems based on the continuous flow (A), multiphase laminar flow (B), batch dilution (C), and zone dispersion (D) methods.

group reported the droplet assembling method and used it to generate droplets with a concentration gradient by aspirating different volumes of sample, reagents, and diluent to form individual droplets under the batch dilution mode (Figure 1C).[29] More recently, Jambovane et al.[30] reported a gradient droplet generation method using a series of microvalves (microfaucets) to control the injected volumes of sample, reagents, and diluent in each droplet. In the above-mentioned systems, the experimental concentration gradients commonly spanned 1−2 orders of magnitude, which could not meet the requirement of enzyme inhibitor screening where concentration gradients with 3−6 orders of magnitude are often needed. Edgar et al.[31] and Niu et al.,[32] respectively, combined the droplet formation technique with capillary electrophoresis and high-performance liquid chromatography (HPLC) separation systems by segmenting the separated component zones into discrete droplets (Figure 1D), which could be used for further treatment and multidimensional separation. Theberge et al.[33] utilized the droplet segmentation of separated component zones eluted from an ultraperformance liquid chromatography (UPLC) system to create a wide range of concentration gradient for each compound in droplet array. In the system, 2 μL of sample containing two components was injected, and a droplet array with concentration gradients of the two components spanning 2−3 orders of magnitude was generated within 40 min. So far, this method has not yet been applied in biological assays. If performing such assays, there may be a limitation that the organic solvents commonly used in HPLC systems, such as methanol or acetonitrile, are not compatible with biological reactions.

In this work, we developed a microfluidic chip-based system for rapidly generating a droplet array with large-scale concentration gradient by coupling flow injection gradient (FIG) technique with droplet microfluidics (Figure 1D). FIG technique is a well-established approach in flow injection analysis (FIA), which was built on the basis of the control of the axial dispersion of injected sample zone in a flowing carrier stream and the acquisition of the concentration gradient information from the whole dispersed sample peak.[34−39] It has advantages of simple operation, high speed, wide concentration gradient, and good compatibility with biological assays and has been successfully applied in automated preparation of sample or reagent solutions with different concentrations,[36] accurate determination of reaction constants,[37,38] and study of drug−protein interactions.[39] In this work, the FIG technique was coupled with droplet-based microfluidics for the first time to generate large-scale concentration gradient in nanoliter-scale droplets with nanoliter sample consumption. By a single injection of 16 nL of sample, an array of droplets with concentration gradient spanning 3−4 orders of magnitude was generated within 2.5 min. The present system not only provides a novel method for generating large-scale concentration gradients in a droplet-based system with extremely low sample consumption and high speed but also contributes to the development of FIG technique. The limitations of conventional FIG systems including dynamic concentration gradient and high sample/reagent consumptions in the microliter range were overcome using the microfluidic droplet segmentation and chip-based FIA techniques. The sample and reagent consumptions were also reduced from microliter to nanoliter range (i.e., 1000 times). In the present system, the slotted-vial array (SVA) technique[40,41] was used to perform automated sample injection and changing and, consequently, achieve automated generation of concentration gradients for different samples. We applied the present system in enzyme inhibition assay to demonstrate its potentials in high-throughput drug screening.

EXPERIMENTAL SECTION

Chemicals. All chemicals used were of analytical grade unless mentioned otherwise, and demineralized water was used throughout. A 10 mM stock solution of sodium fluorescein (Sangon Biotechnology, Shanghai, China) was prepared in 10 mM Tris buffer (pH 7.3), and a series of fluorescein standard solutions were prepared by diluting the stock solution with the buffer sequentially. A 0.5 mg/mL stock solution of β-galactosidase (β-gal, *Escherichia coli*, 248 units/mg, Sigma, St. Louis, MO) was prepared in 10 mM Tris buffer with 0.10 mM $MgCl_2$ (pH 7.3). The inhibitor solutions of 2-phenylethyl β-D-thiogalactoside (PETG, Sigma, St. Louis, MO) and diethylenetriaminepentaacetic acid (DTPA, Nanxiang Reagent Co., Shanghai, China) were prepared and diluted with the same buffer. A 10 mM stock solution of substrate fluorescein digalactoside (FDG, Molecular Probes, Eugene, OR) was prepared in dimethyl sulfoxide (DMSO). Tetradecane (Sigma, St. Louis, MO) was used as oil phase.

Chip Fabrication and Surface Modification. The microchip channel design is shown in Figure S1. (See Supporting Information.) The microchip was fabricated using standard photolithographic, wet chemical etching and bonding techniques as described elsewhere.[42,43] The channel depth and width were 30 and 150 μm, respectively. An on-chip sampling probe was fabricated as described previously.[44] The surface of the microchannel was modified to be hydrophobic using 2% octadecyltrichlorosilane dissolved in toluene (v/v), and the outer surface of the sampling probe was also silanized to reduce the carryover during sample introduction process. (See Supporting Information for details.)

Droplet Concentration Gradient System. As shown in Figure 2, the present system consists of a microchip performing sample injection, reagent mixing, concentration gradient generation, droplet formation, and in-droplet reaction; an automated sample introduction system based on the SVA technique;[40,41] a fluid driving system; and a fluorescence detection system. The slotted vials were fabricated as described elsewhere.[40] The slotted vials for samples and carrier were fixed horizontally on a translational stage under control of a

dx.doi.org/10.1021/ac2029198 | *Anal. Chem.* 2012, 84, 446−452

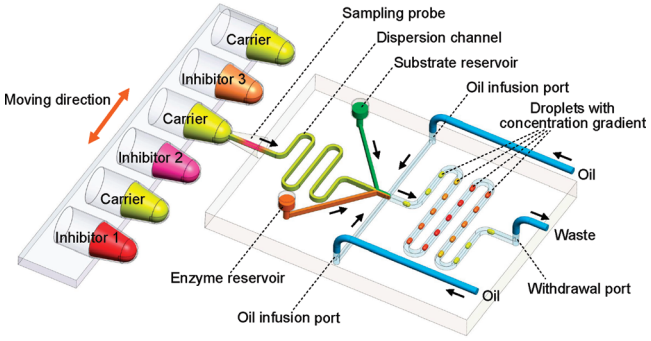

Figure 2. Schematic diagram of the droplet-based microfluidic flow injection gradient analysis chip (not to scale).

computer program. Two syringe pumps (PHD 2000, Harvard Apparatus, Holliston, MA) were used for liquid driving. One pump was used to control the total withdrawal rate $V_{withdrawal}$, while the other was for controlling the oil infusion rate V_{oil}. Gastight syringes (Hamilton, 500 μL) were connected to the microchip via Tygon tubings. A home-built confocal laser induced fluorescence (LIF) detection system was employed for the detection of droplet fluorescence. (See Supporting Information for details.) For direct viewing and recording of the droplet generation process, a stereoscopic zoom microscope (SMZ1500, Nikon, Japan) equipped with a CCD camera (Phantom 663, Vision Research Inc., Wayne, NJ) was used.

Procedures. For enzyme inhibition assays, the sample vials were filled with inhibitor solutions of 4.0 mM DTPA and 1.25 mM PETG, and the carrier vials were filled with 10 mM Tris buffer (pH 7.3). The enzyme and substrate reservoirs were filled with 0.125 mg/mL β-gal and 200 μM FDG solutions, respectively. The operation procedure is shown in Figure 3. Sample injection was performed by linearly moving the translational stage, allowing the sampling probe to sequentially enter the sample and carrier vials for definite residence times to introduce the inhibitor and carrier solutions into the chip channel (Figure 3A). The injected inhibitor zone was dispersed in the flowing carrier stream in the axial direction of the channel, forming a peak-shaped concentration gradient profile (Figure 3B). The dispersed inhibitor zone merged with the substrate and enzyme streams at the first junction of the channel and then was segmented into droplets at the second channel junction by oil phase (Figure 3C). The inhibitor was mixed and reacted with the substrate and enzyme in the droplets, and the reaction product was detected by the LIF system.

Percent activity (%) was calculated using the following equation:[45]

$$\text{Percent activity}\,(\%) = \frac{S_i - S_b}{S_0 - S_b} \times 100\% \qquad (1)$$

where S_b is the signal intensity of background, S_0 is the signal intensity produced without inhibitor, and S_i is the signal intensity with inhibitor. The data of percent activity versus inhibitor concentration were fitted to the sigmoidal dose–response curve[46,47] with Origin 7.5 to obtain the IC_{50} value (inhibitor concentration for 50% inhibition).

Gradient Calibration. We used the relative time-based method to calibrate the concentration gradient, which was widely used in the conventional FIG systems.[48,49] Briefly, a calibration curve between the concentrations of calibrator

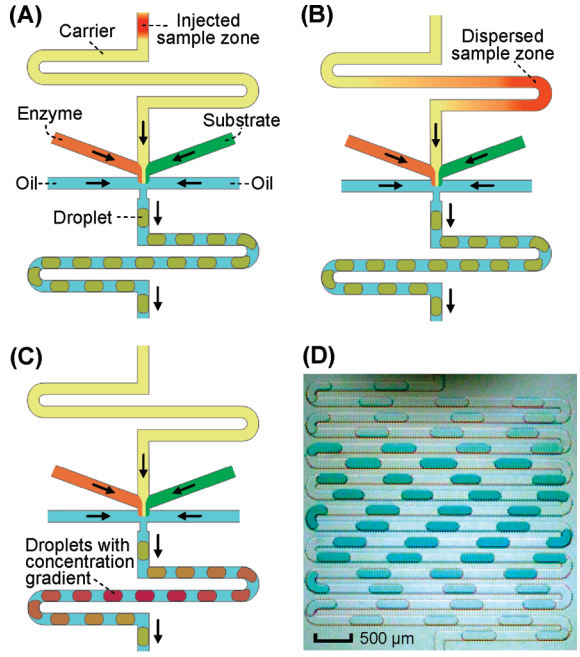

Figure 3. (A–C) Schematic diagram of the generation process of droplet array with concentration gradient by combining the flow injection gradient technique with droplet-based microfluidics. (D) CCD image obtained in the experiment illustrating the principle of the generation of droplet array with concentration gradient. Brilliant blue solution (20 mg/mL) was used as a model sample.

solutions (sodium fluorescein) and their fluorescence intensities was first obtained by sequentially introducing a series of fluorescein standard solutions with a concentration range of 10 nM–80 μM into the chip channel. Then, 1.0 mM fluorescein solution was injected and measured at the same conditions as sample assay. The flow-out curve of droplet fluorescence intensity versus flow-out time showed a typical flow injection (FI) peak profile (Figure 6B). The fluorescein concentration in each droplet in the peak could be obtained with the calibration curve. The relative time of each droplet ($t - t_{max}$), i.e., the difference between the analysis time of each droplet (t) and the time at the FI peak maximum (t_{max}), was calculated individually. The dispersion coefficient ($D_{t-t_{max}}$) of fluorescein in each droplet, indicating the dilution extent of fluorescein in the droplet, was calculated according to the following equation:[50,51]

$$D_{t-t_{max}} = \frac{C_0}{C_{t-t_{max}}} \qquad (2)$$

where C_0 is the original fluorescein concentration of the injected calibrator solution and $C_{t-t_{max}}$ is the fluorescein concentration in the droplet measured at relative time of $t - t_{max}$. A typical curve of dispersion coefficient versus relative time is shown in Figure 5, which clearly exhibited the concentration gradient distribution in the FI peak profile. In the enzyme inhibition assay, since the inhibitor samples were injected and measured under the same conditions, the dispersion coefficient curve could be used to calibrate the concentration gradients of the inhibitor samples. The detailed calibration procedure is provided in Supporting Information.

dx.doi.org/10.1021/ac2029198 | Anal. Chem. 2012, 84, 446–452

RESULTS AND DISCUSSION

Generation of Droplet Array with Concentration Gradient. Our objective is to develop a droplet-based microfluidic system capable of generating droplet arrays with a broad range of concentrations with minimal sample and reagent consumptions, which is specially required in an enzyme inhibition assay for high-throughput drug screening. The FIG technique is capable of generating a wide range of concentrations with high reproducibility, high speed, and relatively low sample consumption.[34−39] Compared with the UPLC-based gradient technique,[33] it has the advantages of simple system structure, low cost, high analysis throughput, and good compatibility with biological assays without the need of organic solvents as carrier. However, in conventional FIG systems, the axial concentration gradient generated in the continuous carrier flow shows dynamic variation with flow time and distance due to the continuous dispersion of sample zone, which presents challenges for applications requiring complicated and relatively slow reactions, such as enzyme inhibition assay. In addition, the conventional FIG systems usually require tens to hundreds of microliters of sample and reagent solutions for a single analysis, which limits the applications where only small amounts (nanoliter to microliter range) of samples and reagents are available. In a previous study, we developed a microchip-based FIA system with sample consumption in the nanoliter range using a capillary sampling probe and a SVA sample presenting system.[40] In this work, we combined the chip-based FIA, droplet-based microfluidics and FIG techniques to build an integrated chip system to achieve nanoliter-scale sample injection, dispersion of injected sample zone (i.e., generation of axial concentration gradient), droplet formation, in-droplet reaction, and online detection. The limitation of dynamic concentration gradients in conventional FIG systems was overcome using a droplet array to segment and preserve the concentration gradient without further dilution and variation. The sample consumption for generating large-scale concentration gradient was also reduced 3 orders of magnitude due to the use of the chip-based FIA system. The operation principle is shown in Figure 3. A sample zone is injected into the sampling probe under FIA mode (Figure 3A) and dispersed in the dispersion channel to form an axial concentration gradient along the channel (Figure 3B). The dispersed sample zone is merged with the reagents and then segmented into an array of droplets by the oil phase in the flow-focusing droplet formation junction (Figure 3C). With the segmentation of the droplets, the concentration gradient profile can be preserved in droplets with high fidelity. Figure 3D shows a CCD image obtained from a video (see Supporting Information) for illustrating the principle of the generation of droplet array with concentration gradient.

Effect of Flow Rates and Injection Volume. In the present system, two syringe pumps connected to the waste port and oil ports were used to control the total withdrawal rate ($V_{withdrawal}$) and the oil infusion rate (V_{oil}), respectively. Therefore, the aqueous flow rate ($V_{aqueous}$) could be expressed as $V_{aqueous} = V_{withdrawal} - V_{oil}$. The aqueous flow was composed of three aqueous streams of sample, enzyme, and substrate, i.e., $V_{aqueous} = V_{sample} + V_{enzyme} + V_{substrate}$. The flow rate ratio of the three aqueous streams was determined by the configurations of the stream channels. With the microchip used in present system, the measured flow rate ratio of sample, enzyme, and substrate streams was 0.35:0.325:0.325.

The effects of $V_{withdrawal}$ on the concentration gradient profile were investigated with a sampling time of 3 s under a fixed aqueous/oil ratio of 1:1. As shown in Figure 4A, the analysis

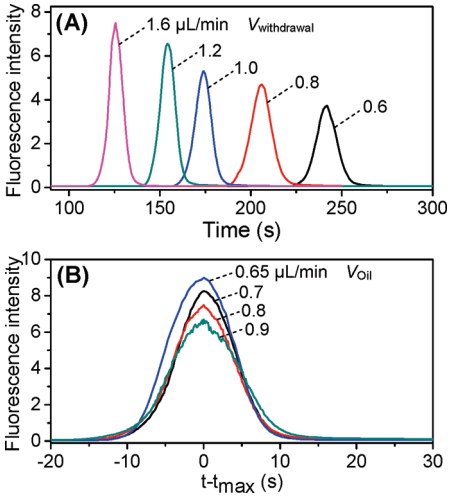

Figure 4. (A) Effects of total withdrawal rate ($V_{withdrawal}$) on concentration gradient profile. Sample injection time: 3 s; Aqueous/oil phase ratio: 1:1. (B) Effects of oil infusion rate (V_{oil}) on concentration gradient profile. $V_{withdrawal}$: 1.6 μL/min; sample injection time: 3 s. Sodium fluorescein (1 mM) was used as a model sample.

time decreased and the peak height increased with the increase of $V_{withdrawal}$ in the range of 0.6−1.6 μL/min. Higher $V_{withdrawal}$ was favorable for decreasing the generation time of the concentration gradient and thus increasing the analysis throughput of the system. However, when the $V_{withdrawal}$ was higher than 2.0 μL/min, air bubbles were easily formed in the pump syringe due to the increase of the flow resistance in the microchannel, which led to unstable $V_{withdrawal}$. Therefore, the flow rate of 1.6 μL/min was selected as $V_{withdrawal}$.

The effects of V_{oil} were studied with a fixed $V_{withdrawal}$ of 1.6 μL/min and a sampling time of 3 s (Figure 4B). The peak heights showed a slight decrease with the increase of V_{oil} in the range of 0.65−0.9 μL/min, which could be attributed to the decrease of sampling volumes caused by the decrease of $V_{aqueous}$. The variation of V_{oil} had evident influence on the droplet formation. When V_{oil} was less than 0.6 μL/min, a multiphase laminar flow consisting of the organic and aqueous streams formed in the channel instead of the segmented flow for the droplet generation. With higher V_{oil}, the peak profiles of the droplet array became rough (Figure 4B). This may be attributed to the increased variation in mixing ratio of the sample and reagent streams under higher droplet formation frequency and smaller droplet size which were caused by the increase of the ratios of $V_{oil}/V_{aqueous}$. Therefore, the oil infusion rate of 0.7 μL/min was chosen.

The effects of the sample injection time at 0.5, 1, 3, 10, and 20 s, corresponding to the injection volume of 2.6, 5.3, 16, 53, and 105 nL, were investigated. The experiment was performed using a sample introduction flow rate V_{sample} of 0.32 μL/min with 1.6, 0.7, 0.29, and 0.29 μL/min for $V_{withdrawal}$, V_{oil}, V_{enzyme}, and $V_{substrate}$, respectively. The peak height increased proportionally with the sample injection time at 0.5−10 s and nearly reached a plateau at 20 s. Although wider concentration gradient ranges could be obtained with longer sampling time, the sample consumption and analysis time also increased. Therefore, the sample injection time of 3 s, corresponding to

dx.doi.org/10.1021/ac2029198 | Anal. Chem. 2012, 84, 446−452

the injection volume of 16 nL, was selected by compromising the sample consumption and the concentration range.

Analytical Performance. We evaluated the performance of the present system in the generation of concentration gradient using sodium fluorescein as a model sample. Figure 5

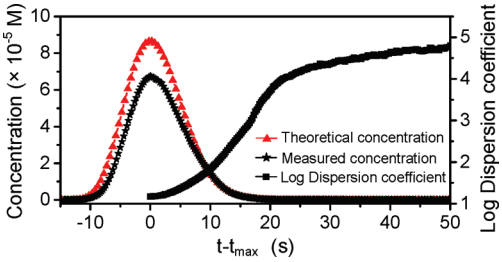

Figure 5. Relationships of the calibrator concentration and log dispersion coefficient with the relative time ($t - t_{max}$). Calibrator: sodium fluorescein, 1 mM; $V_{withdrawal}$: 1.6 μL/min; V_{oil}: 0.7 μL/min; sample injection time: 3 s.

shows a typical concentration gradient profile versus relative time ($t - t_{max}$) with an injection volume of 16 nL of fluorescein solution (1 mM). The maximum and minimum concentrations at the peak profile that could be simultaneously detected by the LIF detection system were 67.5 μM and 15.6 nM at relative times of 0 and 50 s, respectively. The corresponding dispersion coefficients calculated from eq 2 were 14.8 and 6.41 × 10^4, respectively. A log dispersion coefficient versus relative time curve is provided in Figure 5 to show a whole profile of the variation of dispersion coefficient. Therefore, the concentration gradient range spanned 3−4 orders of magnitude, which is higher than those in previously reported droplet-based gradient generation systems.[24−30,33] Since this concentration range was limited by the detection limit and dynamic range of the LIF detector, we used Comsol Multiphysics (Comsol 3.5a, Stockholm, Sweden) to predict the theoretical profile and range of the concentration gradient (Figure 5). The theoretical concentration gradient could range from 830 pM to 86 μM spanning 5 orders of magnitude. The slight deviation between the theoretical and experimental curves may be attributed to the difference of the channel configurations between the actual chip and the theoretical simulation model, since the simulation was carried out on the basis of two-dimensional channel configuration. We also evaluated the performance of the relative time-based calibration method for gradient calibration by repeatedly injecting the fluorescein solution for five times (Figure 6A). The RSD data for the average concentration versus the relative time ($t - t_{max}$) are shown in Figure 6C. The RSD value is 2.2% at 0 s and then gradually increases to the maximum value of 26% at 13.5 s and finally decreases to ca. 10% after 22 s. Nevertheless, these RSD values are still acceptable for enzyme inhibition assays with a major objective for screening.

In the above experiment, the total sample consumption and the gradient generation time for each cycle were 16 nL and 2.5 min, both of which are significantly improved compared with the UPLC-based gradient system.[33]

Enzyme Inhibition Assays. A preliminary study for applying the droplet-based concentration gradient system in enzyme inhibition assay was carried out to demonstrate its potential in high throughput drug screening. The assay was based on the inhibition of β-gal with two model inhibitors, PETG and DTPA, impeding the conversion of FDG to fluorescein mono-D-galactopyranoside and fluorescein. Figure 7A1,B1 shows two typical recordings of the enzyme inhibition assays. More than 240 enzyme inhibition reactions with different inhibitor concentrations spanning 3−4 orders of magnitude were performed in droplets with an extremely low inhibitor injection volume of 16 nL. The concentration gradients of the inhibitors in droplets were calibrated using the relative time-based calibration method, and the percent activity was calculated with eq 1. Figure 7A3,B3 shows the percent activity data for PETG and DTPA at different inhibitor concentrations as well as the corresponding fitted curves in the inhibitor concentration ranges of 0.54−94 μM and 6.9−258 μM, respectively. The average IC_{50} values obtained from three repetitive inhibition assays (Figure S3, Supporting Information) were 18.6 ± 2.9 μM and 120.1 ± 7.6 μM for PETG and DTPA, respectively.

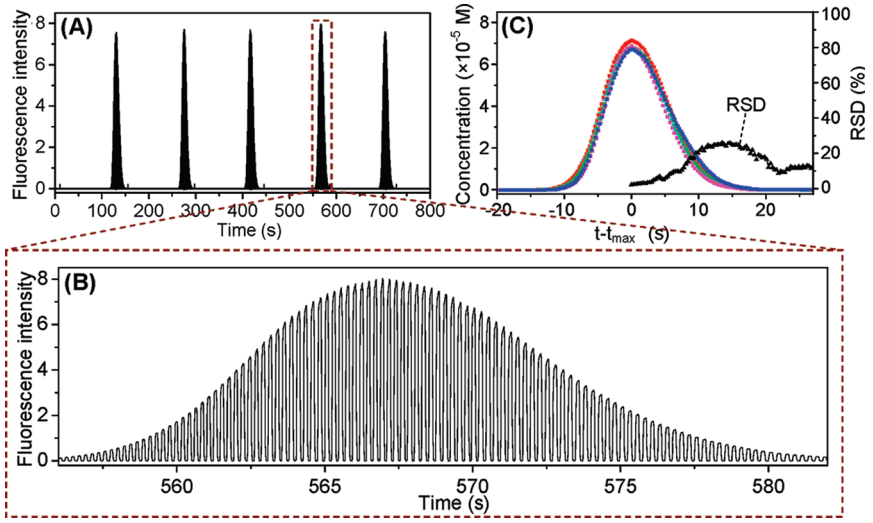

Figure 6. (A) Typical recordings of the fluorescence signal peak profiles obtained with five consecutive injections of fluorescein solution. (B) Enlarged profile of the concentration gradient in the fourth injection of (A). (C) The measured fluorescein concentrations and their RSDs in the individual droplets versus the relative time obtained from data of (A). Conditions are the same as in Figure 5.

dx.doi.org/10.1021/ac2029198 | Anal. Chem. 2012, 84, 446−452

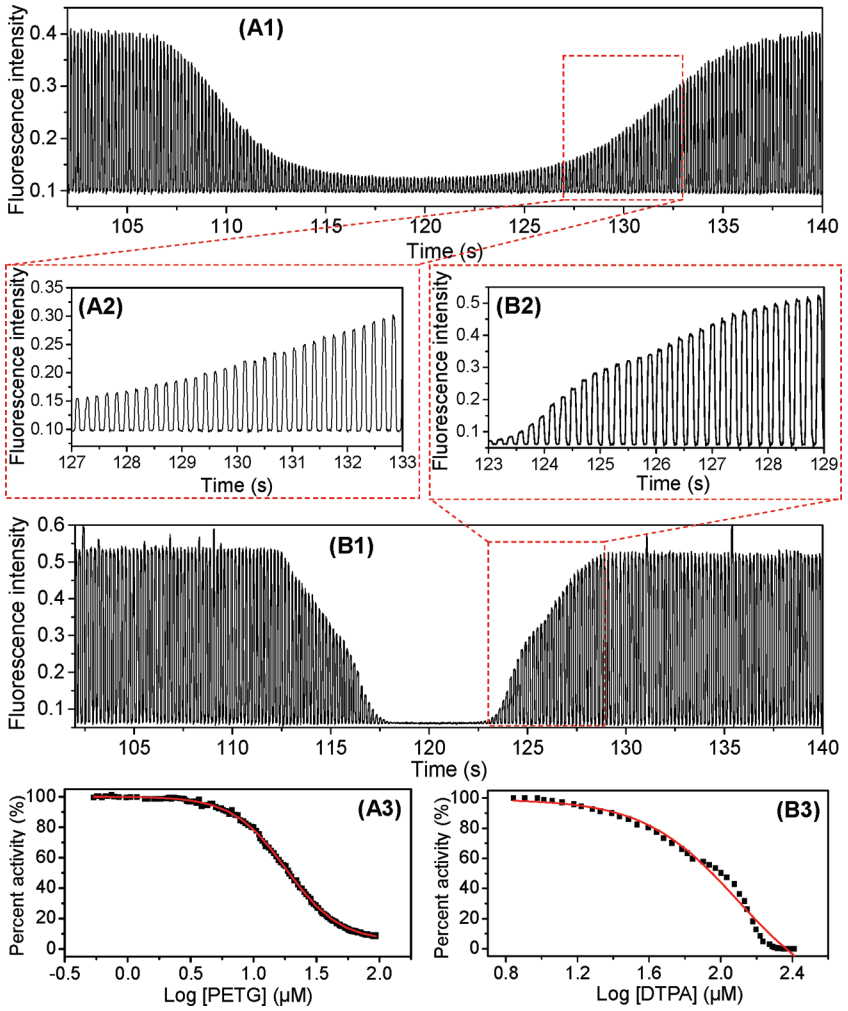

Figure 7. Enzyme inhibition assays with the present droplet-based flow injection gradient analysis system. (A1 and B1) Typical recordings of enzyme inhibition assay for 1.25 mM PETG (A1) and 4 mM DTPA (B1), obtained in one single injection, respectively. (A2 and B2) Enlarged recordings of (A1) in 127−133 s and (B1) in 123−129 s. (A3 and B3) Percent activity data for PETG and DTPA at different inhibitor concentrations as well as the corresponding fitted curves, obtained from (A1) and (B1), respectively. Enzyme: β-galactosidase, 0.125 mg/mL; substrate: fluorescein digalactoside, 200 μM. Other conditions are the same as in Figure 5.

CONCLUSION

We developed a droplet-based system capable of generating droplet array with large-scale concentration gradient by coupling the FIG technique with droplet-based microfluidics. The successful application in the enzyme inhibition assay demonstrated its potential in high throughput drug screening. Compared with traditional multiwell plate-based screening systems, the sample consumption in the present system was reduced 1000-fold. Even compared with microfluidic concentration gradient systems under modes A and B,[24−28] the sample consumption was also significantly reduced more than 100-fold. Using the integrated microchip with multiple modules, the whole operations were achieved within 2.5 min on a single microchip, including valveless nanoliter-scale sample injection, sample zone dispersion, generation of concentration gradient spanning 3−4 orders of magnitude, reagent merging, droplet formation, in-droplet reaction, and online droplet detection. Thus, such a design could significantly simplify the liquid handling operation and improve the throughput of the screening system. In addition, the range of concentration gradient can be further increased using a detection system with higher dynamic range and higher sensitivity. The present system can be applied not only in the enzyme inhibition assay but also in other research fields requiring concentration gradients, such as enzyme kinetics study,[28,30] investigation of drug/protein and protein/protein interactions,[39] and optimization of protein crystallization.[52]

One limitation of the present system is that the precision of relative time-based gradient calibration method is relatively lower than those in conventional FIG systems, which could be attributed to the variation of flow rates in the multiphase droplet system. The calibration precision could be improved using the fluorescent internal standard-based calibration method. With this method, a fluorescent calibrator with a different emission wavelength from that of the product should be added to the sample solution as an internal standard, and a dual-wavelength LIF detector is required to measure the fluorescence intensities of the internal calibrator and the product in droplets simultaneously. Since the added internal calibrator solution has the exact same dispersion conditions as the sample solution, the sample concentration gradient in droplets can be accurately calibrated using the gradient information of the internal calibrator.

dx.doi.org/10.1021/ac2029198 | *Anal. Chem.* 2012, 84, 446−452

■ ASSOCIATED CONTENT

Supporting Information

Additional information as noted in the text. This material is available free of charge via the Internet at http://pubs.acs.org.

■ AUTHOR INFORMATION

Corresponding Author

*Address: Chemical Experiment Building, Room 101, Zhejiang University (Zijingang Campus), Hangzhou 310058, China. Tel: +86-571-88206771. Fax: +86-571-88273572. E-mail: fangqun@zju.edu.cn.

■ ACKNOWLEDGMENTS

The first two authors contributed equally to this work. The authors thank Dr. Xiao-Tong Shi for checking and polishing the writing of the paper. Financial support from National Natural Science Foundation of China (Grants 20825517 and 20890020), Ministry of Science and Technology of China (Grants 2007CB714503 and 2007CB914100), and the Fundamental Research Funds for the Central Universities of China is gratefully acknowledged.

■ REFERENCES

(1) Thorsen, T.; Roberts, R. W.; Arnold, F. H.; Quake, S. R. *Phys. Rev. Lett.* **2001**, *86*, 4163−4166.
(2) Song, H.; Chen, D. L.; Ismagilov, R. F. *Angew. Chem., Int. Ed.* **2006**, *45*, 7336−7356.
(3) Li, L.; Nachtergaele, S.; Seddon, A. M.; Tereshko, V.; Ponomarenko, N.; Ismagilov, R. F. *J. Am. Chem. Soc.* **2008**, *130*, 14324−14328.
(4) Srisa-Art, M.; deMello, A. J.; Edel, J. B. *Anal. Chem.* **2007**, *79*, 6682−6689.
(5) He, M.; Edgar, J. S.; Jeffries, G. D. M.; Lorenz, R. M.; Shelby, J. P.; Chiu, D. T. *Anal. Chem.* **2005**, *77*, 1539−1544.
(6) Shim, J.; Olguin, L. F.; Whyte, G.; Scott, D.; Babtie, A.; Abell, C.; Huck, W. T. S.; Hollfelder, F. *J. Am. Chem. Soc.* **2009**, *131*, 15251−15256.
(7) Clausell-Tormos, J.; Lieber, D.; Baret, J. C.; El-Harrak, A.; Miller, O. J.; Frenz, L.; Blouwolff, J.; Humphry, K. J.; Köster, S.; Duan, H.; Holtze, C.; Weitz, D. A.; Griffiths, A. D.; Merten, C. A. *Chem. Biol.* **2008**, *15*, 427−437.
(8) Ahn, K.; Agresti, J.; Chong, H.; Marquez, M.; Weitz, D. A. *Appl. Phys. Lett.* **2006**, *88*, 264105.
(9) Mazutis, L.; Baret, J. C.; Treacy, P.; Skhiri, Y.; Araghi, A. F.; Ryckelynck, M.; Taly, V.; Griffiths, A. D. *Lab Chip* **2009**, *9*, 2902−2908.
(10) Roach, L. S.; Song, H.; Ismagilov, R. F. *Anal. Chem.* **2005**, *77*, 785−796.
(11) Courtois, F.; Olguin, L. F.; Whyte, G.; Bratton, D.; Huck, W. T. S.; Abell, C.; Hollfelder, F. *ChemBioChem* **2008**, *9*, 439−446.
(12) Wu, N.; Zhu, Y.; Brown, S.; Oakeshott, J.; Peat, T. S.; Surjadi, R.; Easton, C.; Leech, P. W.; Sexton, B. A. *Lab Chip* **2009**, *9*, 3391−3398.
(13) Huebner, A.; Srisa-Art, M.; Holt, D.; Abell, C.; Hollfelder, F.; deMello, A. J.; Edel, J. B. *Chem. Commun.* **2007**, 1218−1220.
(14) Dittrich, P. S.; Jahnz, M.; Schwille, P. *ChemBioChem* **2005**, *6*, 811−814.
(15) Brouzes, E.; Medkova, M.; Savenelli, N.; Marran, D.; Twardowski, M.; Hutchison, J. B.; Rothberg, J. M.; Link, D. R.; Perrimon, N.; Samuels, M. L. *Proc. Natl. Acad. Sci. U.S.A.* **2009**, *106*, 14195−14200.
(16) Pei, J.; Li, Q.; Kennedy, R. T. *J. Am. Soc. Mass Spectrom.* **2010**, *21*, 1107−1113.
(17) Clausell-Tormos, J.; Griffiths, A. D.; Merten, C. A. *Lab Chip* **2010**, *10*, 1302−1307.
(18) Pei, J.; Nie, J.; Kennedy, R. T. *Anal. Chem.* **2010**, *82*, 9261−9267.
(19) Mugherli, L.; Burchak, O. N.; Balakireva, L. A.; Thomas, A.; Chatelain, F.; Balakirev, M. Y. *Angew. Chem., Int. Ed.* **2009**, *48*, 7639−7644.
(20) Wong, E.; Okhonin, V.; Berezovski, M. V.; Nozaki, T.; Waldmann, H.; Alexandrov, K.; Krylov, S. N. *J. Am. Chem. Soc.* **2008**, *130*, 11862−11863.
(21) Dertinger, S. K. W.; Chiu, D. T.; Jeon, N. L.; Whitesides, G. M. *Anal. Chem.* **2001**, *73*, 1240−1246.
(22) Kamholz, A. E.; Weigl, B. H.; Finlayson, B. A.; Yager, P. *Anal. Chem.* **1999**, *71*, 5340−5347.
(23) Mao, H. B.; Cremer, P. S.; Manson, M. D. *Proc. Natl. Acad. Sci. U.S.A.* **2003**, *100*, 5449−5454.
(24) Song, H.; Ismagilov, R. F. *J. Am. Chem. Soc.* **2003**, *125*, 14613−14619.
(25) Li, L.; Mustafi, D.; Fu, Q.; Tereshko, V.; Chen, D. L.; Tice, J. D.; Ismagilov, R. F. *Proc. Natl. Acad. Sci. U.S.A.* **2006**, *103*, 19243−19248.
(26) Lorenz, R. M.; Fiorini, G. S.; Jeffries, G. D. M.; Lim, D. S. W.; He, M; Chiu, D. T. *Anal. Chim. Acta* **2008**, *630*, 124−130.
(27) Damean, N.; Olguin, L. F.; Hollfelder, F.; Abell, C.; Huck, W. T. S. *Lab Chip* **2009**, *9*, 1707−1713.
(28) Bui, M. P. N; Li, C. A.; Han, K. N.; Choo, J.; Lee, E. K.; Seong, G. H. *Anal. Chem.* **2011**, *83*, 1603−1608.
(29) Du, W. B.; Sun, M.; Gu, S. Q.; Zhu, Y.; Fang, Q. *Anal. Chem.* **2010**, *82*, 9941−9947.
(30) Jambovane, S.; Kim, D. J.; Duin, E. C.; Kim, S. K.; Hong, J. W. *Anal. Chem.* **2011**, *83*, 3358−3364.
(31) Edgar, J. S.; Milne, G.; Zhao, Y.; Pabbati, C. P.; Lim, D. S. W.; Chiu, D. T. *Angew. Chem., Int. Ed.* **2009**, *48*, 2719−2722.
(32) Niu, X. Z.; Zhang, B.; Marszalek, R. T.; Ces, O.; Edel, J. B.; Klug, D. R.; deMello, A. J. *Chem. Commun.* **2009**, 6159−6161.
(33) Theberge, A. B.; Whyte, G.; Huck, W. T. S. *Anal. Chem.* **2010**, *82*, 3449−3453.
(34) Betteridge, D.; Fields, B. *Anal. Chem.* **1978**, *50*, 654−656.
(35) Ruzicka, J.; Hansen, E. H. *Anal. Chim. Acta* **1979**, *106*, 207−224.
(36) Clark, G. D.; Ruzicka, J.; Christian, G. D. *Anal. Chem.* **1989**, *61*, 1773−1778.
(37) Georgiou, M. E.; Georgiou, C. A.; Koupparis, M. A. *Anal. Chem.* **1995**, *67*, 114−123.
(38) Tran, C. D.; Baptista, M. S.; Tomooka, T. *Langmuir* **1998**, *14*, 6886−6892.
(39) Georgiou, M. E.; Georgiou, C. A.; Koupparis, M. A. *Anal. Chem.* **1999**, *71*, 2541−2550.
(40) Du, W. B.; Fang, Q.; He, Q. H.; Fang, Z. L. *Anal. Chem.* **2005**, *77*, 1330−1337.
(41) Sun, M.; Fang, Q. *Lab Chip* **2010**, *10*, 2864−2868.
(42) Fang, Q.; Xu, G. M.; Fang, Z. L. *Anal. Chem.* **2002**, *74*, 1223−1231.
(43) Jia, Z. J.; Fang, Q.; Fang, Z. L. *Anal. Chem.* **2004**, *76*, 5597−5602.
(44) Zhu, Y.; Pan, J. Z.; Su, Y.; He, Q. H.; Fang, Q. *Talanta* **2010**, *81*, 1069−1075.
(45) Motlekar, N.; Diamond, S. L.; Napper, A. D. *Assay Drug Dev. Technol.* **2008**, *6*, 395−405.
(46) Rathore, R.; Pribil, P.; Corr, J. J.; Seibel, W. L.; Evdokimov, A.; Greis, K. D. *J. Biomol. Screening* **2010**, *15*, 1001−1007.
(47) Green, L. S.; Bullard, J. M.; Ribble, W.; Dean, F.; Ayers, D. A.; Ochsner, U. A.; Janjic, N.; Jarvis, T. C. *Antimicrob. Agents Chemother.* **2009**, *53*, 86−94.
(48) Gisin, M.; Thommen, C.; Mansfield, K. F. *Anal. Chim. Acta* **1986**, *179*, 149−167.
(49) Fan, S. H.; Fang, Z. L. *Anal. Chim. Acta* **1990**, *241*, 15−22.
(50) Hungerford, J. M.; Christian, G. D.; Ruzicka, J.; Giddings, J. C. *Anal. Chem.* **1985**, *57*, 1794−1798.
(51) Ruzicka, J.; Hansen, E. H. *Anal. Chim. Acta* **1983**, *145*, 1−15.
(52) Zheng, B.; Roach, L. S.; Ismagilov, R. F. *J. Am. Chem. Soc.* **2003**, *125*, 11170−11171.